Mechanical investigation of solid MNs penetration into skin using finite element analysis

Tianqi Liu [a,b], Yanfang Sun [c], Wenjing Zhang [a], Rui Wang [a,b], Xinyu Lv [a], Lei Nie [d], Amin Shavandi [e], Khaydar E. Yunusov [f], Guohua Jiang [a,b,*]

[a] *School of Materials Science and Engineering, Zhejiang Sci-Tech University, Hangzhou, 310018, China*

[b] *International Scientific and Technological Cooperation Base of Intelligent Biomaterials and Functional Fibers, Hangzhou, 310018, China*

[c] *College of Life Sciences and Medicine, Zhejiang Sci-Tech University, Hangzhou, Zhejiang, 310018, China*

[d] *College of Life Sciences, Xinyang Normal University, Xinyang 464000, China*

[e] *Université libre de Bruxelles (ULB), École polytechnique de Bruxelles, 3BIO10 BioMatter, Avenue F.D. Roosevelt, 50 - CP 165/61, 1050 Brussels, Belgium*

[f] *Institute of Polymer Chemistry and Physics, Uzbekistan Academy of Sciences, Tashkent, 100128, Uzbekistan*

[g] *Research Institute for Physical Chemical Problems of the Belarusian State University, Minsk, 220030, Belarus*

E-mail: ghjiang_cn@zstu.edu.cn (G. Jiang)

Abstract: In the past two decades, MNs patches (MNs) as a promising platform have been extensively investigated for transdermal delivery of drug drugs, cells, and active substances and extraction of bio-fluids. To realize painless, efficacious and safe transdermal delivery, these MNs must penetrate the skin to the appropriate depth without breaking or bending. Therefore, effective prediction of mechanical properties such as skin penetration of microneedles is crucial for the material and structural design of MNs. In this paper, a numerical simulation of the insertion process of the microneedle into various types of skin modeling is reported using the finite element method. The effective stress failure criterion has been coupled with the element deletion technique to predict the complete insertion process. The numerical results show a good agreement with the reported experimental data for the deformation and failure of the skin and the insertion force.

Keyword: Microneedles; transdermal delivery; insertion forces; skin mechanics

1. Introduction

Blood sampling, diagnosis and drug delivery, as components of the medical treatment system, have played an essential role in therapeutic practices.[1] Over the past hundred years, conventional steel injection needles have been widely used for blood sampling and transdermal delivery of drugs due to the perfect skin penetration. Nevertheless, the pain and invasiveness associated with penetration of needles through the skin are resisted.[2]

To overcome the limitations of steel injection needles, microneedles (MNs) as a novel transdermal delivery technology composed of needles on the micrometer scale, which have been extensively studied for replacing traditional steel injection needles due to their painless, non-invasive, self-administered properties.[3] In the last two decades, MNs have been used to deliver vaccines,[4] peptides,[5] proteins,[6] small molecule drugs,[7] cells,[8] which exhibiting the potential alternative route for drug delivery. In addition, MNs can also avoid cross-infection caused by injection use, reducing the risk of cross-infection in medical care. With the development of MNs technology and microelectronic technology, MNs have also been studied for blood and tissue fluid (ISF) extraction and point-of-care (POC) medical tests, avoiding the frequent use of steel injection needles. [9-11]

Currently, different types (solid MNs, hollow MNs, coated MNs, dissolvable MNs and hydrogel MNs) and structures of MNs have been designed for various applications.[12-13] The insertion process of MNs into tissue, however, remains a complex and challenging issue due to the highly non-linear and nonlinearly

inhomogeneous nature of the needle and tissue.[14] The interaction between the needle and tissue, loading conditions, and material properties will affect the insertion forces, stress and strain distributions, and needle deformation during the insertion process.[15] Therefore, the modeling and simulation of MNs insertion can provide critical insight into the mechanics of MNs and tissue interaction, and contribute to optimize the design of MNs-based devices for various medical applications.

At present, there are different methods to predict the MNs insertion procedure including dye immersion staining,[16] fluorescence diffusion,[17] and embedding in tissue sections.[18] The dye immersion staining and fluorescence diffusion to assess MNs penetration could be affected by temperature of skin.[19] Furthermore, in the case of optimal cutting temperature compound (OCT) embedding, embedding skin samples is a necessary step which may cause the displacement of MNs from their original location, thereby compromising the accuracy of measurement.[20-21] Mathematical simulation of the MN systems is an area of growing research where the theories governing drug transport and delivery through the skin can be suitably applied for the development and optimisation of MN systems. In addition, an accurate finite element model can provide a detailed analysis of the stress micro-environment during MNs array insertion, which can be used to predict insertion performance and to efficiently compare the impact of design feature modifications.

A variety of studies have been conducted in response to different procedures of MNs insertion. The shape of the MNs has a great influence on the penetration of the MNs. Common conical MNs have been designed and simulated by COMSOL

Multiphysics software, exhibiting less stress and easier insertion into the skin compared with pyramidal MNs.[22] In addition, a variety of novel MNs have been designed by CAD and analyzed by the COMSOL Multiphysics software. Flanged base was added to the design to the base of MNs reduce stress and fracture.[23] The length of MNs has a great effect on the penetration process, and excessively long MNs can pierce the skin, whereas too short MNs cannot resist the elasticity of skin and thus cannot pierce the skin.[24] Longer MNs can deliver drugs to deeper concluded in both simulation experiments and animal experiments.[25] However, it should be noted that the length of MNs should not be increased excessively, as excessively long MNs may lead to skin damage and pain. It has been investigated the feasibility of microneedles with various lengths penetrating the skin, and determined that a length of 550-900 μm is optimal for effective skin penetration.[26] "The nail bed effect" poses a challenge to MNs patch design, as it necessitates a suitable density of MNs. However, a recent study utilizing a 3D finite element analysis model developed with Abaqus software has shown that reducing the density of MNs can actually enhance MNs penetration depth and efficiency.[27] New MNs structures and optimized parameters (such as needle tip area and MNs wall thickness) have the potential to further reduce the force required for MNs insertion. [28-31] By exploring these design factors, the penetration efficiency and patient compliance of MNs can be improved.

The interaction between MNs and skin can be comprehended by simulating the process of MNs insertion into the skin using COMSOL software. This simulation enables the optimization of MNs' structures, thereby enhancing their skin insertion

performance. By evaluating the MNs insertion, potential issues such as stress concentration, fracture, and skin damage can be identified and mitigated, leading to improved safety and reliability of the MNs. In addition, MNs with superior mechanical strength require minimal force for successful skin penetration. The minimum force necessary for MNs to insert the skin under different conditions can be simulated by COMSOL software, providing a valuable guidance for MNs' materials and structure designs.

Here, we presented a novel finite element model for simulating conical MNs to insert into skin. The skin model incorporates multiple viscoelastic, anisotropic layers to accurately reflect skin conditions *in vivo*. The effects of different insertion speeds, needle acuity, needle tip area, needle spacing, and skin thickness on the insertion of MNs into the skin were simulated by finite element modeling (Figure 1). In addition, the effect of pre-treatment of the skin during the insertion process on MNs insertion has also been investigated. The numerical results show a good agreement with the reported experimental data for the deformation and failure of the skin and the insertion force, which can be suitably applied for the materials and structure optimisation of MN systems in the future.

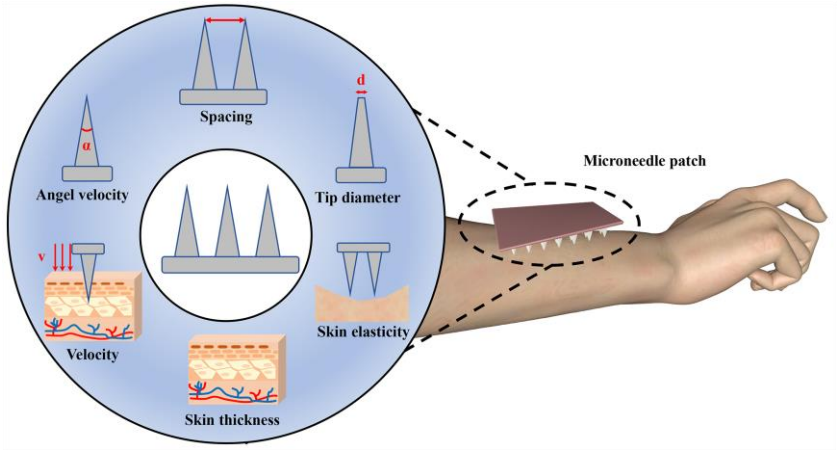

Figure 1. Schematic representation of different factors to affect the insertion of MNs.

2. Finite element modeling

The finite element models were created in COMSOL Multiphysics (Comsol Multiphysics 6.1, America). Solid mechanics module added stainless steel was chosen as the material of various MNs models to ensure that the MNs had sufficient mechanical strength to explore the optimal conditions for insertion to the skin. The specific material selected is "Structural steel" with a density of 7850 kg/m^3 in the Comsol software. In this model, MNs were designed to have 700 μm hight, 200 μm ground surface diameter, which could be adjusted to other sizes upon request. In addition, The MNs patch (5×5) model with the same backing and different spacing was also designed to evaluate the effect of MNs spacing on MNs insertion.

The skin model established was a multi-layered material comprising stratum corneum (~ 20 μm), epidermis (~ 80 μm) and dermis (~ 1 mm) layers to simulate the skin as accurately as possible (Figure 2A). Stiff stratum corneum, the main obstacle to the insertion process, was modeled with the Neo-Hookean model. The dermis layer was further molded with Gasser-Ogden-Holzapfel (GOH) in the Neo-Hookean model. The calculation method for volumetric strain energy is Miehe. Meanwhile, the contact

pairs between the MNs and the skin were added, and the effect of adhesion and stripping was added. The friction coefficient in the model was set to be 0.42 controlled by the penalty factor.[32] Specific parameters adopted in the model in each skin layer are shown in the Table 1. In addition, the 'contact' was set up at the interfaces between different layers to assemble cohesively to produce a integrated skin without the occurrence of gaps. The MNs as the source object was set to be a finer meshing, while the skin as the target object was set to be extremely refined to make both contacts instead of traversing. Among them, the shear stiffness in adhesion is defined using the shear normal ratio (0.17), while the cohesive force model for delamination is based on displacement damage. Additionally, fixed constraints are applied to the lower surface of the dermis to secure the entire skin, thus facilitating the process of insertion. The stress cloud plot of the model was used to analyze the data to evaluate the effects of factors such as the speed of penetration, MNs acuity, needle tip area, needle spacing, skin thickness, and skin tension on the MNs entry process.

Table 1 Mechanical properties of the skin model [27,33]

	Stratum corneum	Epidermis	Dermis
Material Model	Neo-hookean	Neo-hookean	Gasser-Ogden-Holzapfel
Thickness (mm)	0.02	0.08	1
Density (g/cm^3)	1.3	1.2	1.2
Youngs modulus (MPa)	0.752	0.489	7.33

3. Results

3.1 Skin tension

Skin is a complex structure that varies significantly in both structure and mechanical properties depending on the species, the individual and the specific site.

Skin tension, which refers to how tensed the skin is when subjected to external forces, is an important factor affecting MNs insertion. The tension of the skin was variable at different locations, which is difficult to control, the same property skin was chosen to simulate the effect of different tension forces on the piercing process. The addition of a roll support to the side of the skin model in the COMSOL software has simulated stretched skin, which corresponds to an increase in tension, as shown in Figure 2B and 2C. In contrast, the skin model without setup of roll support mimics the skin in natural condition is shown in Figure 2B and 2D. Both of the MNs systems with roll supported and no roll supported groups were pierced into the skin at a velocity of 1 $mm \cdot s^{-1}$. Utilizing the above simulation system, the effect of skin tension on MNs entry can be analyzed qualitatively. Here, the setting of the roller support is slightly different from the practical stretching of the skin. In practical applications, the skin is subjected to direct stretching by applying a specific force. When roller support is added to the skin, it does not generate any tension in the absence of MNs penetration force. However, the skin with roller support will generate the same tension as the skin to prevent skin deformation during the MNs penetration, which can still meet the evaluation of various stretching situations.

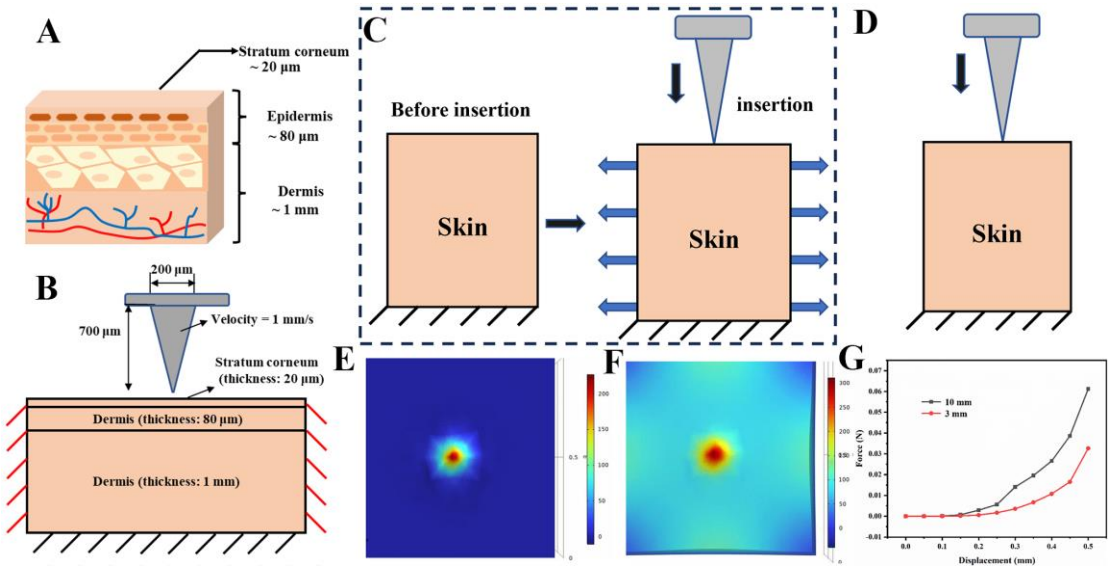

Figure 2. Schematic of the skin structure (A), insertion illustration of MNs on skin (B), insertion illustration of MNs and top stress distribution clouds on stretched skin (C and E) and non-stretched skin (D and F). Force displacement curve of roller support set at distances of 3 mm and 10 mm (G).

The orthogonal and positive views of the roller supported skin piercing situation are shown in Video 1 and Video 2, which has the minimal deformations and tremors during penetration. In contrast, the skin without roll support undergoes a significant deformation during the stab in process according to the orthogonal and positive views in Video 3 and Video 4. The stretching of the skin can change the morphological and mechanical properties of the skin, which can enhance the penetration depth of MNs and improve the insertion efficiency of MNs as well. The stress distribution clouds in Figure 2E and 2F show that the maximum stresses skin with and without roll support are 2.5×10^4 and 4.5×10^4 Pa, respectively. As compared to the stress exerted on skin with roller support during MNs insertion, the stress without roller support is significantly greater. This stress difference can be attributed to the presence of uneven skin and higher friction without the support of a roller. In addition, the setting distance of the roller support has an impact on the penetration. In Figure 2G, it can be observed

that the force exerted on the roller support set at 10 mm is considerably higher than that on the roller support set at 3 mm, particularly after a displacement of 200 μm. This suggests a correlation between the roller support distance and the required force, with greater distances necessitating increased force. This phenomenon could potentially be attributed to the enhanced elasticity of the skin, which is a consequence of the increased distance.

3.2 Velocity of insertion

To evaluate the effect of speed on the penetration of MNs into the skin, the MNs model at the same depth at which different velocity (velocity = 0.1, 0.3, 0.5, 0.7, 1, 1.3, 1.5 $mm \cdot s^{-1}$) into the skin. Figure 3A shows the definition of the boundary conditions for the MNs insertion. The thickness of stratum corneum and dermis are set at 20 and 1000 μm, respectively. And the conical MNs, with height and bottom diameter at 700 and 200 μm, and angle of MNs tip at 20°, are vertically penetrated into the skin under a constant velocity. When the velocity controlled at 0.1 $mm \cdot s^{-1}$, the maximum bearing force at axial direction for the MNs is ~0.147 N/needle during the insertion process. And increasing the velocity to ~0.3 $mm \cdot s^{-1}$ and 0.5 $mm \cdot s^{-1}$, the maximum bearing force for the MNs insertion can be decreased to ~ 0.120 and 0.054 N/needle, showing a rapid decrease trend with the velocity ranging from 0.1 to 0.5 $mm \cdot s^{-1}$. However, further increasing the velocity from ~0.5 $mm \cdot s^{-1}$ and 1.5 $mm \cdot s^{-1}$, the maximum bearing force decreases from ~0.054 to 0.017 N/needle, showing a relatively gentle decrease trend (Figure 3B). With an increase in speed from 0.1 $mm \cdot s^{-1}$ to 1.5 $mm \cdot s^{-1}$, there is a corresponding decrease in radial force from 0.689

mN/needle to 0. 083 mN/needle. The trend is similar to Olatunji 's work [34], where they used a copolymer of methyl vinyl ether and maleic anhydride (PMVE-MA) to mold conical MNs. When the insertion rate increased from 0.5 mm s^{-1} to 1 mm s^{-1} and the penetration force decreased from 0.03 N to 0.0216 N. At the same time, there is also a similar trend when using MNs applicators in practice, even if there are differences in numerical values due to different usage conditions [35-36]. Thus, the MNs with a lower insertion velocity is beneficially reduces the initial insertion force due to the elastic characteristics of the skin. Generally, MNs withstanding insertion force more than 0.1 N/needle can be effectively inserted into the skin.

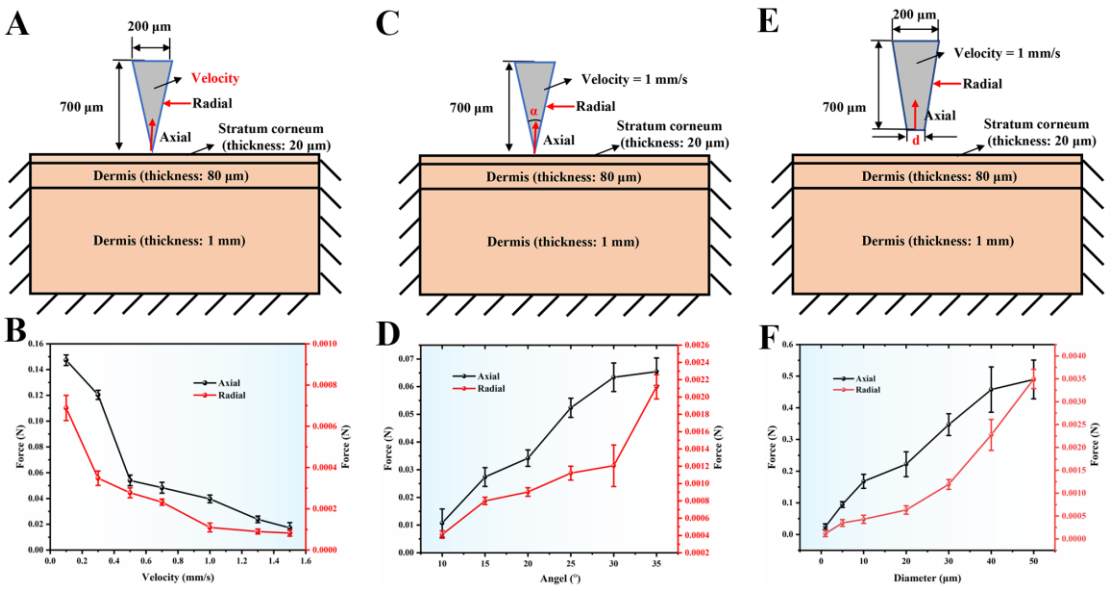

Figure 3. Definition of the boundary conditions for MNs insertion (A), and axial and radial insertion force of MNs into skin at different velocity (B). Definition of the boundary conditions for MNs insertion (C), and axial and radial insertion forces of MNs with different needle tip angles (D). Definition of the boundary conditions for MNs insertion (E), and axial and radial insertion forces of MNs with different needle tip diameters (F).

3.3 Angle of MNs tips

The angle of the MNs tip indicates the sharpness degree of the needle tip. Here, the relationship between insertion force and the angle of the needle tip are also

investigated. MNs models with different needle tip angles (a = 10°, 15°, 20°, 25°, 30° and 35°) are applied to the skin models, as shown in Figure 3C. The conical MNs, with height and bottom diameter at 700 and 200 μm, are vertically penetrated into the skin under a constant velocity at 1.0 $mm \cdot s^{-1}$. When the angle of the MNs tip at 10°, the axial and radial forces are 0.011 N/needle and 0.0004 N/needle. Increasing the angle of the MNs tip to 20°, the axial and radial forces are increased to 0.034 N/needle and 0.001 N/needle, respectively. Further increasing the angle of the MNs tip to 35°, the axial and radial forces are increased to 0.065 and 0.002 N/needle. Essentially, MNs with lower tip angles is best configured for insertion (Figure 3D). The above phenomena can be explained that the larger the angle of the needle tip means the larger the area of the needle body and, consequently, the greater the pressure, friction, as well as shear forces. To reduce the MNs insertion force and improve the insertion efficiency, reducing the needle tip angle is an important parameter, however a smaller angle also means a smaller drug loading, which requires a balance.

3.4 Diameter of MNs tips

The effect of the needle tip on the insertion force of the MNs is investigated by setting different needle tip diameters (d = 1, 5, 10, 20, 30, 40 and 50 μm), as shown in Figure 3E. All MNs insert the skin model at a velocity of 1 mm/s with respective tip diameters. As expected, the insertion force will be increased with increasing the tip diameter of needle. The insert force is 0.025 N/needle when the diameter of the MNs tip at 1 μm. It will be enhanced to 0.168 N/needle with the diameter of the MNs tip at 10 μm, about ~6.72 times higher than that of the MNs tip diameter at 1 μm. However,

only ~1.32 times enhancement (~0.222 N/needle) can be obtained with increasing the diameter of the MNs tip to 20 μm. Further increasing the diameter of the MNs tip to 40 and 50 μm, the insert forces are 0.458 N/needle and 0.490 N/needle, respectively. The MNs radial force for a needle tip diameter ranging from 1 μm to 20 μm increases from 0.117 mN to 0.633 mN, followed by a faster increase from 0.633 mN to 3.50 mN within the range of 20 μm to 50 μm. (Figure 3F). Thus, the higher insert force will be endowed with the larger needle tip diameter. The penetration force of the metal hollow MNs measured by Ranamukhaarachchi has the same trend, and as the needle tip area increases, the penetration force and energy force increase [37]. It should be noticed the skin tissue damage will be caused to extend the skin healing time.

3.5 Spacing of the needles

The spacing of MNs in an array are critical determinant of skin penetration and the mechanical integrity of the MNs. To evaluate the effect of spacing of MNs on penetration efficiency in skin, the MNs with 700 μm in height and 200 μm in bottom diameter with difference spacing (10, 50, 100, 200, 400, and 800 μm) are designed to simulate the MNs insertion at velocity of 1.0 $mm \cdot s^{-1}$, as shown in Figure 4A.

Figure 4B shows the cloud plot of stress distribution for MNs insertion. The interactive stress effects of the MNs cannot be clearly distinguished in the clouds plot of stress distribution when MNs spacing varying from 10 to 100 μm. Upon increasing the spacing beyond 200 μm, the stress distribution becomes dispersed and a visible gap emerges, indicating a reduced stress interaction among the MNs. Figure 4D shows the plot relations between of penetration depth and efficiency with interval

spacing of MNs. When the interval spacing of MNs at 10 μm, the penetration depth and efficiency are 469 μm and 87.5%, respectively. And they will be enhanced to 521 μm and 99.4% when increased interval spacing of MNs to 200 μm. However, the penetration depth and efficiency are almost no signature changed after further increasing the interval spacing of MNs. There is no significant increase in insertion depth when the interval spacing of MNs increased to 800 μm. To observe the stress distribution of different MNs spacing more clearly, Figure 4C shows the top view of the stress distribution cloud map of the skin model. As the spacing between MNs increases, the stress during the process of insert into the skin becomes more dispersed. These findings suggest that MNs spacing above 200 μm may be necessary to reduce mutual stress and enhance the performance of skin penetration.

The similar trend also can be found between the insertion force and interval spacing of MNs. Figure 4E shows the displacement distribution cloud plots against the interval spacing of MNs. And the corresponding insertion force curves are dispalyed in Figure 4F. There are no significant alterations can be observed in the skin displacement and penetration depth when the interval spacing of MNs controlled at 10, 50, and 100 μm. And the required penetration force is 0.49, 0.23 and 0.22 N/Needle. It indicated that the required stronger penetration force is need for the MNs with smaller interval spacing. By further increasing the interval spacing of MNs, the required insertion force becomes weaker, with only approximately 0.063 N/needle needed for insertion. However, the change in the required penetration force becomes insignificant when the interval spacing of MNs exceeds 200 μm. These findings are consistent with

the results of Olatunji's work,[34] showing that the spacing of needle only begins to affect insertion force at low spacing (< 150 μm). This range of needle spacing is also consistent with the conclusion of Römgens's work, proving that appropriate needle spacing is beneficial for drug delivery and diffusion [38]. Therefore, we believe that optimizing interval spacing of MNs is a crucial factor for enhancing the insertion of MNs patches.

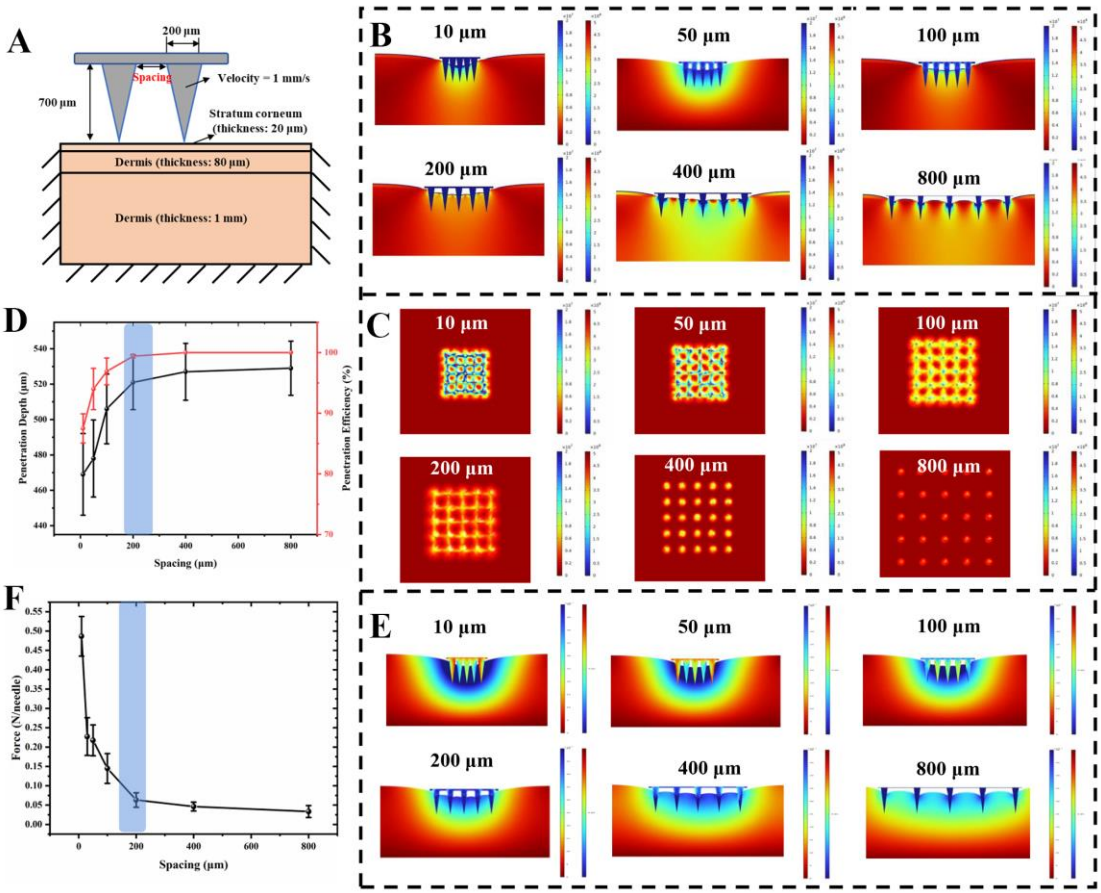

Figure 4. Definition of the boundary conditions for MNs insertion with different interval spacing (A). Cross section (B) and top view (C) of stress distribution cloud plot against interval spacing and penetration depth and efficiency of MNs with different spacings (D). Displacement distribution cloud plot against interval spacing (E) and insertion forces changes at different interval spacing (F).

3.6 Thickness of the skin

The stratum corneum, as the outermost layer of the skin surface, is also the main barrier to skin penetration, and the thickness of the stratum corneum is usually

between 10-20 μm due to effect of different locations and age. [39-40] The flow of MNs into each layer of the skin is shown in Figure 5. The MNs do not develop any stress when MNs are only contacted with the skin (Figure 5A). And the stress will be enhanced when the MNs are pressed on the stratum corneum, and they will be punctured into skin when the stress exceeds the elastic modulus of the skin (Figure 5B), and subsequent penetration into the epidermal layer (Figure 5C). Therefore, the penetration force of MNs will be affected by the thickness of the stratum corneum and epidermis. To further investigate the efficacy of MNs insertion into different skin thicknesses, various parameters are modified in the stratum corneum and epidermis layer of the skin model. And changes in skin thickness are simulated by subjecting the skin model to a series of MNs penetrations, allowing for a comprehensive evaluation of application of MNs patches across a broad range of skin thicknesses (Figure 5D).

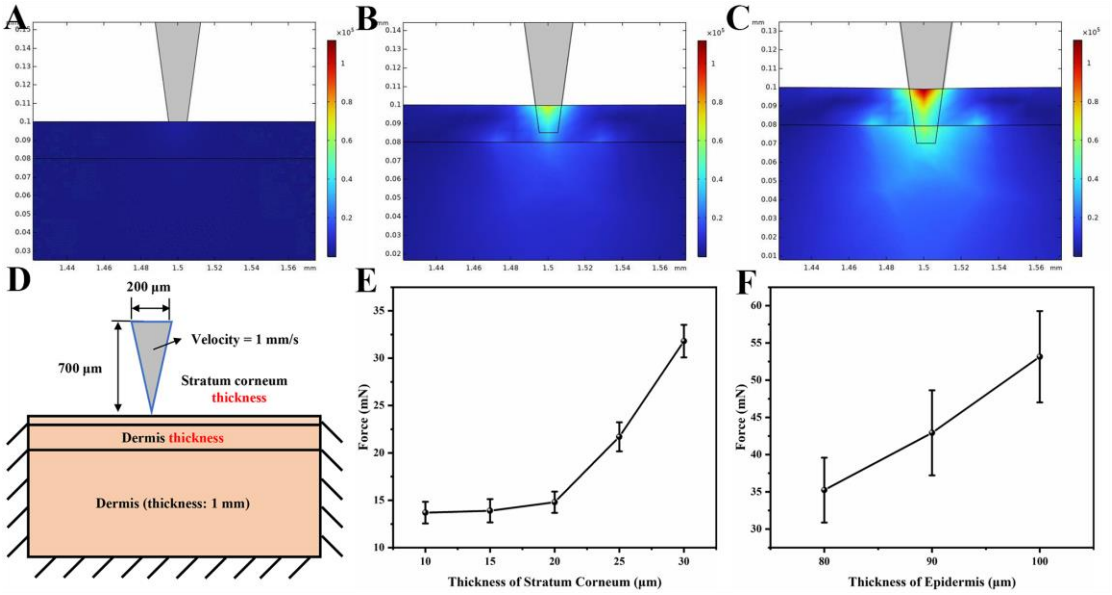

Figure 5. MNs on the surface of skin model before insertion (A), Insertion of MNs into the stratum corneum (B) and epidermal layers (C). Definition of the boundary conditions with different thickness of stratum corneum and epidermal layers (D). Effect of stratum corneum thickness (E) and epidermal thickness on MNs insertion (F).

As shown in Figure 5E, the resistance for MNs insertion will be increased with

increasing thickness of the stratum corneum. And the insertion force is increased by 123.6 % from 0.014 N to 0.033 N as the thickness of stratum corneum increasing from 10 μm to 30 μm. In addition, the thickness of the epidermal layer has a similar trend of influence. The insertion force of the MNs is 35.2 mN when the thickness of the epidermal layer controlled at 80 μm. And the insertion force of the MNs will be improved to 53.1 mN when the thickness of the epidermal layer at 100 μm (Figure 5F).

4. Conclusion

In conclusion, a finite element model has been developed for simulating conical MNs to insert into skin. The skin model incorporates multiple viscoelastic, anisotropic layers to accurately reflect skin conditions *in vivo*. In this study, the effects of of pre-treatment of the skin during the insertion process on MNs insertion and other insertion parameters including insertion speeds, needle acuity, needle tip area, needle spacing, and skin thickness were simulated and assessed by finite element modeling. The numerical results show a suitable needle insertion velocity (> 0.7 $mm \cdot s^{-1}$), needle tip diameter (< 10 μm), and needle spacing (> 200 μm) can effectively reduce the needle insertion force of MNs. To conclude, the finite element model developed can be used as a tool to optimize MNs construct design and predict MNs puncture efficacy.

Declaration of Competing Interest

The authors declare that they have no known competing financial interests or personal relationships that could have appeared to influence the work reported in this paper.

Acknowledgments

This work was financially supported by the Huadong Medicine Joint Funds of the Zhejiang Provincial Natural Science Foundation of China under Grant No. LHDMZ23H300003 and the National Natural Science Foundation of China under Grant No. 51873194.

References

[1] Vahid Ebrahiminejad, Philip D. Prewett, Graham J. Davies, Zahra Faraji Radm, MNs Arrays for Drug Delivery and Diagnostics: Toward an Optimized Design, Reliable Insertion, and Penetration, Advanced Materials Interfaces, 2022, 9:2101856.

[2] Rigved Nagarkar, Mahima Singh, Hiep X. Nguyen, Sriramakamal Jonnalagadda, A review of recent advances in MNs technology for transdermal drug delivery, Journal of Drug Delivery Science and Technology, 2020, 59: 101923.

[3] Tianqi Liu, Guohua Jiang, Gao Song, Yanfang Sun, Xueya Zhang, Zhiyong Zeng, Fabrication of rapidly separable MNs for transdermal delivery of metformin on diabetic rats, Journal of Pharmaceutical Sciences, 2021, 110(8): 3004-3010.

[4] Khanh T. M. Tran, Tyler D. Gavitt, Nicholas J. Farrell, Eli J. Curry, Arlind B. Mara, Avi Patel, Lindsey Brown, Shawn Kilpatrick, Roxana Piotrowska, Neha Mishra, Steven M. Szczepanek, Thanh D. Nguyen, Transdermal microneedles for the programmable burst release of multiple vaccine payloads, Nature Biomedical Engineering, 2021, 5: 998-1007.

[5] Colin Dillon, Helen Hughes, Niall J. O'Reilly, Chris J. Allender, David A. Barrow, Peter Mcloughlin, Dissolving MNs based transdermal delivery of therapeutic peptide analogues, International Journal of Pharmaceutics, 2019, 565(30): 9-19.

[6] Yanqi Ye, Jicheng Yu, Di Wen, Anna R. Kahkoska, Zhen Gu, Polymeric MNs for transdermal protein delivery, Advanced Drug Delivery Reviews, 2018, 127-1: 106-118.

[7] Tianqi Liu, Yanfang Sun, Guohua Jiang, Wenjing Zhang, Rui Wang, Lei Nie,

Amin Shavandi, Khaydar E. Yunusov, Uladzislau E. Aharodnikau, Sergey O. Solomevich, Porcupine-inspired MNs coupled with an adhesive back patching as dressing for accelerating diabetic wound healing, Acta Biomaterialia, 2023, 160: 32-44.

[8] Yujuan Zhu, Shiyuan Li, Yifan Li, Hui Tan, Yuanjin Zhao, Lingyun Sun, Antioxidant nanozyme MNs with stem cell loading for in situ endometrial repair, Chemical Engineering Journal, 2022, 449(1): 137786.

[9] Peng Xue, Lei Zhang, Zhigang Xu, Junjie Yan, Zhen Gu, Yuejun Kang, Blood sampling using MNs as a minimally invasive platform for biomedical diagnostics, Applied Materials Today, 2018, 13: 144-157.

[10] Rongyan He, Yan Niu, Zedong Li, Ang Li, Huayuan Yang, Feng Xu, Fei Li, A hydrogel MNs patch for point-of-care testing based on skin interstitial fluid, Advanced Healthcare Materials, 2020, 9(4): 1901201.

[11] Xianlei Li, Xuehui Xu, Kewei Wang, Yuqiu Chen, Yangyuchen Zhang, Qingrui Si, Zi'an Pan, Fan Jia, Xinyue Cui, Xuan Wang, Xiongwei Deng, Li Zhao, Dan Shu, Qiao Jiang, Baoquan Ding, Yan Wu, Ran Liu, Fluorescence-amplified origami MNs (FAOM) device for quantitatively monitoring blood glucose, Advanced Materials, 2023, 2208820.

[12] Tianqi Liu, Guohua Jiang, Gao Song, Jiangying Zhu, Yuhui Yang, Fabrication of separable MNs with phase change coating for NIR-triggered transdermal delivery of metformin on diabetic rats, Biomedical Microdevices, 2020, 22: 12.

[13] Rui Wang, Guohua Jiang, Uladzislau E. Aharodnikau, Khadar Yunusov, Yanfang

Sun, Tianqi Liu, Sergey O. Solomevich, Recent advances in polymer MNs for durg transdermal delivery: design strategies and applications, Macromolecular Rapid Communications, 2022, 43(8): 2200037.

[14] Pooyan Makvandi, Melissa Kirkby, Aaron R. J. Hutton, Majid Shabani, Cynthia K. Y. Yiu, Zahra Baghbantaraghdari, Rezvan Jamaledin, Marco Carlotti, Barbara Mazzolai, Virgilio Mattoli, Ryan F. Donnelly, Engineering MNs patches for improved penetration: analysis, skin models and factors afecting needle insertion, Micro & Nano Letters, 2021, 13: 93.

[15] Xueliang Xiu, Guangzhi Gao, Yong Liu, Fengsen Ma, Drug delivery with dissolving MNs: skin puncture, its influencing factors and improvement strategies, Journal of Drug Delivery Science and Technology, 2022, 76:103653.

[16] Han Sol Lee, Ha Ryeong Ryu, Joo Young Roh, Jung-Hwan Park, Bleomycin-coated MNs for treatment of warts, Pharmaceutical Research, 2016, 34: 101-112.

[17] Rui Wang, Han Wang, Guohua Jiang, Yanfang Sun, Tianqi Liu, Lei Nie, Amin Shavandi, Khaydar E Yunusov, Uladzislau E Aharodnikau, Sergey O Solomevich, Transdermal delivery of allopurinol on acute gout rats via polymer MNs for regulation of blood uric acid levels, Biomaterials Science, 2023, 11: 1704-1713.

[18] Zhiyong Zeng, Guohua Jiang, Yanfang Sun, Uladzislau E Aharodnikau, Khaydar E Yunusov, Xiaofei Gao, Tianqi Liu, Sergey O Solomevich, Rational design of flexible MNs coupled with CaO_2@PDA-loaded nanofiber films for skin wound healing on diabetic rats, Biomaterials Science, 2022, 10: 5326-5339.

[19] S. A. Ranamukhaarachchi, S. Lehnert, S. L. Ranamukhaarachchi, L. Sprenger, T. Schneider, I. Mansoor, K. Rai, U. O. Häfeli, B. Stoeber, A micromechanical comparison of human and porcine skin before and after preservation by freezing for medical device development, Scientific Reports, 2016, 6 (1): 32074.

[20] Shayan F. Lahiji, Manita Dangol, Hyungil Jung, A patchless dissolving MNs delivery system enabling rapid and efficient transdermal drug delivery, Scientific Reports, 2015, 5(1): 7914.

[21] Zheyu Wang, Jingyi Luan, Anushree Seth, Lin Liu, Minli You, Prashant Gupta, Priya Rathi, Yixuan Wang, Sisi Cao, Qisheng Jiang, Xiao Zhang, Rohit Gupta, Qingjun Zhou, Jeremiah J Morrissey, Erica L Scheller, Jai S Rudra, Srikanth Singamaneni, MNs patch for the ultrasensitive quantification of protein biomarkers in interstitial fluid, Nature Biomedical Engineering, 2021, 5(1): 64–76.

[22] Gowthami Anbazhagan, Sreeja Balakrishnapillai Suseela, Radha Sankarajan, Design, analysis and fabrication of solid polymer MNs patch using CO2 laser and polymer molding, Drug Delivery and Translational Research, 2023, 13: 1813-1827.

[23] Zahra Faraji Rad, Robert E. Nordon, Carl J. Anthony, Lynne Bilston, Philip D. Prewett, Ji-Youn Arns, Christoph H. Arns, Liangchi Zhang, Graham J. Davies, High-fidelity replication of thermoplastic MNs with open microfluidic channels, Microsystems & Nanoengineering, 2017, 3: 17034.

[24] Ryan F. Donnelly, Martin J. Garland, Desmond I.J. Morrow, Katarzyna Migalska, A. David Woolfson, Optical coherence tomography is a valuable tool in the study of the effects of MNs geometry on skin penetration characteristics and in-skin

dissolution, Journal of Controlled Release, 2010, 147(3): 333-341.

[25] Adam Davidson, Barrak Al-Qallaf, Diganta Bhusan Das, Transdermal drug delivery by coated MNs: geometry efects on efective skin thickness and drug permeability, Chemical Engineering Research and Design, Chemical Engineering Research and Design, 2008, 86(11): 1196-1206.

[26] F. J. Verbaan, S. M. Bal, D. J. van den Berg, W. H. H. Groenink, H. Verpoorten, R. Luttge, J. A. Bouwstra, Assembled MNs arrays enhance the transport of compounds varying over a large range of molecular weight across human dermatomed skin. Journal of Controlled Release, 2007, 117(2): 238-245.

[27] Wenting Shu, Helen Heimark, Nicky Bertollo, Desmond J. Tobin, Eoin D. O'Cearbhaill, Aisling Ní Annaidh, Insights into the mechanics of solid conical MNs array insertion into skin using the finite element method, Acta Biomaterial, 2021, 135: 403-413.

[28] X.Q. Kong, P. Zhou, C.W. Wu, Numerical simulation of MNs' insertion into skin, Computer Methods in Biomechanics and Biomedical Engineering, 2011, 14(9): 827-835.

[29] Puneet Khanna, Kevin Luongo, Joel A Strom, Shekhar Bhansali, Sharpening of hollow silicon MNs to reduce skin penetration force, Journal of Micromechanics and Microengineering, 2010, 20:045011.

[30] Md Asadujjaman Sawon, Mst Fateha Samad, Design and optimization of a MNs with skin insertion analysis for transdermal drug delivery applications, Journal of Drug Delivery Science and Technology, 2021, 63: 102477.

[31] Hafzaliza Erny Zainal Abidin, Poh Choon Ooi, Teck Yaw Tiong, Noraini Marsi, Abrar Ismardi, Mimiwaty Mohd Noor, Nik Amni Fathi Nik Zaini Fathi, Norazreen Abd Aziz, Siti Kudnie Sahari, Gandi Sugandi, Jumril Yunas, Chang Fu Dee, Burhanuddin Yeop Majlis, Azrul Azlan Hamzah, Journal of Pharmaceutical Sciences, 2020, 109(8): 2485-2492.

[32] Ahmed Elkhyat, Carol Courderot-Masuyer, Tijani Gharbi, Philippe Humbert, Influence of the hydrophobic and hydrophilic characteristics of sliding and slider surfaces on friction coefficient: in vivo human skin friction comparison, Skin Research & Technology, 2004, 10(4): 215–221.

[33] Shuhu Chen, Nannan Li, Jing Chen, Finite element analysis of MNs insertion into skin, Micro & Nano Letters, 2012, 7(12): 1206-1209.

[34] Ololade Olatunji, Diganta B. Das, Martin J. Garland, Luc Belaid, Ryan F. Donnelly, Influence of array interspacing on the force required for successful MNs skin penetration: theoretical and practical approaches. Journal of Pharmaceutical Sciences, 2013, 102(4): 1209-1221.

[35] Geonwoo Kang, Minkyung Kim, Huisuk Yang, Jiwoo Shin, Jeeho Sim, Hyeri Ahn, Mingyu Jang, Youseong Kim, Hye Su Min, Hyungil Jung, Latch applicator for efficient delivery of dissolving microneedles based on rapid release of elastic strain energy by thumb force, Advanced Functional Materials, 2023, 33(11): 2210805.

[36] Mara Leone, Bart H. van Oorschot, M. Reza Nejadnik, Andrea Bocchino, Matteo Rosato, Gideon Kersten, Conor O'Mahony, Joke Bouwstra, Koen van der Maaden, Universal applicator for digitally-controlled pressing force and impact velocity

insertion of microneedles into skin, Pharmaceutics, 2018, 10: 211.

[37] Sahan A. Ranamukhaarachchi, Boris Stoeber, Determining the factors affecting dynamic insertion of microneedles into skin, Biomedical Microdevices, 2019, 21: 100.

[38] Anne M. Römgens, Dan L. Bader, Joke A. Bouwstra, Cees W. J. Oomens, Predicting the optimal geometry of microneedles and their array for dermal vaccination using a computational model, Computer Methods in Biomechanics and Biomedical Engineering, 2016, 19(15): 1599-1609.

[39] Aisling Ní Annaidh, Karine Bruyère, Michel Destrade, Michael D. Gilchrist, Mélanie Otténio, Characterization of the anisotropic mechanical properties of excised human skin, Journal of the Mechanical Behavior of Biomedical Materials, 2012, 5(1): 139-148.

[40] Desmond J. Tobin, Introduction to skin aging, Journal of tissue viability, 2017, 26(1): 37-46.